Intercompartmental Electron Exchange in Geometrically-Constrained Ru−Os Triads Built around Diethynylated Aryl Hydrocarbons

Abdelkrim El-ghayoury,[†] Anthony Harriman,*[,‡] and Raymond Ziessel[†]

Laboratoire de Chimie, d'Electronique et Photonique Moléculaires, Ecole Européenne de Chimie, Polymères et Matériaux, Université Louis Pasteur, 25 rue Becquerel, F-67087 Strasbourg Cedex 02, France, and Department of Chemistry, University of Newcastle, Newcastle upon Tyne NE1 7RU, U.K.

Received: February 21, 2000; In Final Form: June 14, 2000

A set of molecular triads has been synthesized in which terminal ruthenium(II) and osmium(II) tris(2,2′-bipyridyl) fragments are separated by a butadiynylene residue bearing a central aromatic nucleus. The aromatic groups are 1,4-phenylene, 1,4-naphthalene, and 9,10-anthracene, and they exert a marked influence on the nature of intramolecular triplet energy-transfer processes involving the terminals. The phenylene unit facilitates long-range energy transfer from the "Ru(bpy)" fragment (bpy = 2,2′-bipyridine) to the corresponding "Os(bpy)" unit. Electron exchange in this system takes place via superexchange interactions with the central phenylene group acting as mediator. Replacing phenylene with naphthalene decreases the triplet energy of the connector such that the naphthalene-like triplet lies at slightly lower energy than the Ru(bpy) fragment but well above the triplet state localized on the Os(bpy) unit. Triplet energy transfer along the molecular axis involves two discrete steps, forming the naphthalene-like triplet as a real intermediate, both of which are fast. The triplet energy of the anthracene-derived connector is lower than that of the Os(bpy) fragment, and this unit acts as an energy sink for photons absorbed by the terminal metal complexes. However, slow energy leakage occurs from the anthracene-like triplet to the Os(bpy) unit, stabilizing the latter triplet state, and providing a means for achieving energy transfer along the molecular axis. The various kinetic results are discussed in terms of intercompartmental energy transfer.

Intramolecular triplet energy transfer over modest distances (e.g., 10−30 Å) has been demonstrated in numerous organic[1] and organometallic systems.[2] Triplet energy transfer usually proceeds via the Dexter electron-exchange mechanism[3,4] and, in rigid or sterically constrained molecules, involves through-bond orbital interactions.[5] According to the nature of the connecting "spacer" framework, electron exchange can be extremely fast[6] or quite slow,[7] while several systems have been found to display reversible triplet energy transfer[8−11] between nearly isoenergetic terminals. It has further been shown that alkynylene groups are highly effective at promoting through-bond electron exchange between metal (M = Ru, Os) polypyridine complexes,[12] having an attenuation factor (β) of ca. 0.17 Å^{-1}, but it is known that such connectors do not couple strongly to phenyl rings also incorporated in the bridge.[13,14] This is unfortunate because phenyl rings provide a simple means by which to vary the solubility, tunability, and length of the bridge. In principle, the barrier to through-bond electron exchange imposed by an interspersed phenylene unit could be eliminated if this latter fragment would operate as a relay[15,16] for triplet energy transfer along the molecular axis. Thus, a two-step process might be expected to provide a faster overall rate of energy transfer than a one-step (i.e., long-range) process[17] but this requires careful matching of the relevant triplet energy levels.

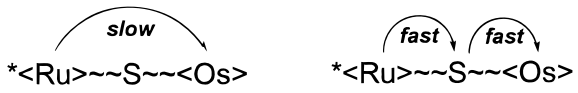

Indeed, it has been shown that multistep Dexter-type singlet energy transfer can be highly effective in porphyrin-based molecular arrays.[18] Two-step triplet energy transfer occurs in certain polymers loaded with ruthenium(II) and osmium(II) polypyridine complexes and bearing pendant anthracene residues as the energy relay.[19] This latter work has stimulated the design of a molecular triad comprising a central anthracene unit and ruthenium(II) and osmium(II) polypyridine complexes as photoactive terminals.[16] Although intramolecular triplet energy transfer occurs from the Ru(bpy) (bpy = 2,2′-bipyridine) fragment to the corresponding Os(bpy) unit with a rate constant of ca. 5×10^8 s^{-1}, the flexible connectors do not eliminate direct contact between the terminals and, as a consequence, the role of the anthracene-based relay remains obscure.[16] This uncertainty could be minimized by using rigid connectors or by designing a molecular triad in which the individual fragments are maintained in a well-defined geometrical arrangement that favors a two-step mechanism. One way to construct such triads is to connect the anthracene unit to the terminal metal complexes via ethynylene groups so as to form a linear array. This arrangement benefits from the excellent electronic conductivity of the carbon bridge[12,20] and from the directionality imposed by the ethynylene substituent that ensures the lowest-energy triplet state localized on each metal complex will involve charge injection from metal center to the functionalized ligand.[21] The other advantage of this approach is that the central aromatic

* Author to whom correspondence should be addressed.
[†] Laboratoire de Chimie, d'Electronique et Photonique Moléculaires, Ecole Européenne de Chimie, Polymères et Matériaux, Université Louis Pasteur.
[‡] Department of Chemistry, University of Newcastle.

10.1021/jp000675o CCC: $19.00
Published on Web 08/01/2000

unit can be substituted with additional groups to assist dispersion in organized media.

In this article we describe intramolecular electron exchange in mixed-metal Ru−Os triads built around different aromatic units but maintaining a fixed geometry.[22] The photophysical properties of the corresponding mono- and binuclear complexes have been described earlier[23] and are used here to establish triplet energy levels. It is shown that the triplet energy of the aromatic unit can be positioned above, below, or between those of the terminal metal complexes. Since the triads are sterically constrained, the mechanism of the energy-transfer process can be resolved in each case. An important general point that should be stressed here is that triplet states associated with the terminal metal complexes are of metal-to-ligand, charge-transfer character but, because of spin−orbital coupling restrictions, may not be pure triplet states. Triplets localized on the bridging polytopic ligand are of π,π^* character and, most likely, closely resemble pure triplet states.

Experimental Section

Materials. Reagent grade solvents and chemicals were used in the synthesis of the mixed-metal Ru−Os complexes. Chromatographic separations were made using neutral alumina (Aldrich, 80−200 mesh) and reagent grade solvents. Synthesis of the various ligands[22] and mononuclear Os(II) complexes[23] followed literature procedures. Preparation of the heterodinuclear complexes was achieved by reacting the appropriate mononuclear Os(II) complex with silver-dehalogenated $Ru(bpy)_2Cl_2$. This solution was prepared by mixing *cis*-$[Ru(bpy)_2Cl_2]\cdot 2H_2O$[24] (1 equiv) and $AgBF_4$ (2 equiv) in argon-degassed ethanol and heating overnight at or near reflux. After cooling to 20 °C, the deep-red solution was filtered over cotton-wool and transferred quantitatively via cannula to an ethanolic solution of the corresponding mono-Os(II) complex (0.5 equiv). After heating at 100 °C for 2 days, the mixture was cooled to 20 °C before addition of KPF_6 (ca. 5-fold-excess) in H_2O (10 mL). Slow evaporation of the organic solvent led to the precipitation of a brownish solid. The precipitate was isolated, washed with water under centrifugation (3 × 10 mL) and diethyl ether (3 × 10 mL), and chromatographed on alumina using a gradient of CH_3OH (1 to 5%) in CH_2Cl_2. The first fraction was discarded and the subsequent highly colored band was collected. Recrystallization from acetone/hexane afforded the required deep-brown complex in an analytically pure state. The complexes were characterized by various spectroscopic techniques, including electrospray-mass spectroscopy, and by elemental analysis. The techniques and apparatus used to characterize all new compounds are detailed elsewhere.[25]

RBPBO: 80%; ($R_f = 0.18$, alumina, CH_2Cl_2/CH_3OH: 95/5, v/v). UV/Vis (CH_3CN): λ_{max}, nm (ϵ, M^{-1} cm^{-1}) 282 (115 600); 358 (68 700); 446 (19 400). IR (KBr pellets): ν, cm^{-1} 2925 (w), 2855 (w), 2224 (w, $\nu_{C\equiv C}$), 1741 (w), 1464 (s), 1266 (m), 840 (s). ES-MS in CH_3CN, *pseudo*-molecular peaks at *m*/*z* 499.0 $[M-3PF_6]^{3+}$, 820.8 $[M-2PF_6]^{2+}$. Anal. Calc. for $C_{70}H_{50}N_{12}RuOsP_4F_{24}$ (*Mr* = 1930.386): C = 43.56; H = 2.61, N = 8.71. Found: C = 43.34; H = 2.52; N = 8.45.

RBNBO: 85%; ($R_f = 0.25$, alumina, CH_2Cl_2/CH_3OH: 95/5, v/v). UV/Vis (CH_3CN): λ_{max}, nm (ϵ, M^{-1} cm^{-1}) 289 (126 800); 446 (27 000); 470 (19 800). IR (KBr pellets): ν, cm^{-1} 2925 (w), 2210 (w, $\nu_{C\equiv C}$), 1600 (w), 1465 (m), 1266 (w), 840 (s). ES-MS in CH_3CN, *pseudo*-molecular peaks at *m*/*z* 515.7 $[M-3PF_6]^{3+}$, 945.8 $[M-2PF_6]^{2+}$. Anal. Calc. for $C_{74}H_{52}N_{12}OsRuP_4F_{24}$ (*Mr* = 1980.166): C = 44.80; H = 2.64; N = 8.49. Found: C = 44.62; H = 2.65; N = 8.49.

RBABO: 50%; ($R_f = 0.22$, alumina, CH_2Cl_2/CH_3OH: 95/5, v/v). UV/Vis (CH_3CN): λ_{max}, nm (ϵ, M^{-1} cm^{-1}) 250 (83 100); 280 (143 600); 469 (43 500). IR (KBr pellets): ν, cm^{-1} 2924 (w), 2195 (w, $\nu_{C\equiv C}$), 1598 (w), 1460 (w), 1403 (w), 1239 (w); 840 (s). ES-MS in CH_3CN, *pseudo*-molecular peaks at *m*/*z* 362.5 $[M-4PF_6]^{4+}$. Anal. Calc. for $C_{78}H_{54}N_{12}OsRuP_4F_{24}$ (*Mr* = 2030.507): C = 46.14; H = 2.68, N = 8.28. Found: C = 45.79; H = 2.63; N = 7.93.

Methods. Absorption spectra were recorded at ambient temperature with a Kontron Instruments Uvikon 930 spectrophotometer. Luminescence spectra were recorded in deoxygenated acetonitrile at 20 °C using a modified Perkin-Elmer LS50 spectrofluorimeter equipped with a silicon photocell as detector operated at 77 K. The emission monochromator was replaced in order to collect data from 500 to 1000 nm and the resultant spectra were corrected for imperfections of the instrument by reference to a standard lamp. Spectra were averaged over 10 runs and the quoted emission maxima were reproducible to within ±5 nm. Quantum yields were calculated relative to ruthenium(II) and osmium(II) tris(2,2′-bipyridyl) complexes in acetonitrile,[26,27] using dilute solutions after deoxygenation by purging with argon. Luminescence quantum yields were taken as the average of three separate determinations and were reproducible to within ±8%.

Luminescence lifetimes were measured with a variety of instruments according to the required time window and excitation wavelength. For **RBPBO**, the sample was illuminated with a 25 ps laser pulse as delivered by a frequency-doubled, mode-locked Nd:YAG laser. The excitation pulse was Raman shifted with water (648 nm to excite the Os(bpy) fragment) or ethanol (460 nm to directly excite both terminals) so as to produce more appropriate excitation wavelengths. Residual 532 nm light was removed with a notch filter and the required beam was passed through a narrow band-pass filter prior to excitation. The laser intensity was attenuated to 5 mJ per pulse, and incident pulses were defocused onto an adjustable pinhole positioned in front of the sample cuvette. Luminescence was collected with a microscope objective lens at 90° to excitation and isolated from any scattered laser light with nonemissive glass cutoff filters. The emergent luminescence was focused onto the entrance slit of a Spex high-radiance monochromator interfaced to a second monochromator and thereby passed to a fast-response photodiode. The output signal was transferred to a Tektronix SCD1000 transient recorder and subsequently to a microcomputer for storage and analysis. Approximately 500 individual laser shots, collected at 10 Hz, were averaged for kinetic measurements. The temporal resolution of this instrument was ca. 0.2 ns. Emission lifetimes measured with this setup were reproducible to within ±5%. All kinetic measurements were made with samples previously deoxygenated by purging with argon, and the absorbance of each solution was adjusted to be ca. 0.08 at the excitation wavelength. Data analysis was made by a nonlinear, least-squares iterative fitting routine that utilized a modified Levenberg−Marquardt global minimization procedure, after deconvolution of the instrument response function.[28]

For **RBNBO**, the sample was excited with a mode-locked, frequency-doubled Nd:YAG laser (Antares 76S) operated at 82 MHz and emission was detected with a synchronous streak camera. A double monochromator, placed between collecting optics and the streak camera, was used to isolate the desired wavelength region. The signal was accumulated, corrected for background illumination and analyzed as above. After deconvolution the temporal resolution of this setup, being limited by trigger jitter, was ca. 15 ps but the available time window was

restricted to <1 ns. The luminescence lifetime of the Os(bpy) fragment was measured as above following excitation at either 648 or 532 nm with a 25 ps laser pulse. This latter setup was also used to monitor emission from the Os(bpy) fragment in **RBABO**. Attempts to measure luminescence from the corresponding Ru(bpy) fragment in **RBABO** following excitation at 532 nm and using the streak camera as detector were unsuccessful, possibly because the bridging ligand absorbs at this wavelength. Likewise, it was not possible to obtain meaningful decay kinetics over the 0−1 ns time range for the Os(bpy) triplet with this instrument.

Laser flash photolysis studies were made using a frequency-doubled, mode-locked Antares 76S pumped dual-jet dye laser operated with Rhodamine 6G (5 mJ, 600 nm). The output beam was split into two parts with approximately 80% and 20% of the total intensity, respectively. The most intense beam was used as the excitation source (FHWM = 350 fs), while the weaker beam was depolarized and focused into a 1 cm cuvette filled with water to produce a white light continuum for use as the analyzing pulse. The continuum was split into two equal beams before reaching the delay stage so as to provide a reference beam by which to normalize the transient absorption spectrum. This reference beam arrived at the sample cell ca. 1 ns before the excitation and analyzing beams; with the latter two pulses passing almost collinearly through the sample. After passing through the sample, these beams were collected by fiber optics and analyzed with an image-intensified, Princeton dual-diode array spectrograph. The spectrometer was operated at 10 Hz, with 100 individual laser shots being averaged at each delay time. Baseline corrections were applied and emission was subtracted from the resultant spectra by recording control signals without the excitation or continuum pulses. Differential absorption spectra were corrected for distortions by reference to the optical Kerr effect obtained from CS_2. Experiments requiring longer time scales were made with a Q-switched Nd:YAG laser (fwhm = 10 ns, 532 or 355 nm, 10 mJ). The monitoring beam was provided by a pulsed, high-intensity Xe arc lamp passed through the sample at 90° to the excitation pulse. Spectra were compiled point-by-point, with 5 individual records being collected at each wavelength, using a Spex high-radiance monochromator operated with 2 nm slits. Kinetic measurements were made at fixed wavelength, with 100 individual laser shots being averaged for each decay profile. All solutions were prepared in deoxygenated acetonitrile so as to provide an absorbance of ca. 0.2 at the excitation wavelength.

Spectral overlap integrals were calculated from normalized absorption and emission spectra recorded for the mononuclear reference compounds in acetonitrile. In estimating the orientation factor it is assumed that the lowest-energy triplet state is formed by selective charge injection into the substituted ligand. As such, a set of 12 pairs of transition dipoles can be considered, for which distances and angles can be estimated from MM2 energy-minimized conformations (Gaussian 98). A rate constant for Förster-type energy transfer was calculated for each pair of transitions and the rates summed to give the global rate constant. Franck−Condon factors for electron exchange were calculated from luminescence spectra using the procedure introduced by Meyer and co-workers,[29] as described previously.[23]

Results and Discussion

Background. The abbreviations used throughout this manuscript can be explained as follows: The metal center is specified as being R [ruthenium(II)] or O [osmium(II)], with the overall charge being neglected. The coordinating ligand is 2,2′-bipyridine [B] while the central aromatic unit is selected from 1,4-phenylene [P], 1,4-naphthalene [N], or 9,10-anthracene [A]. For the mixed-metal binuclear complexes, all five structural units are specified (e.g., **RBPBO**) but only three units are given for

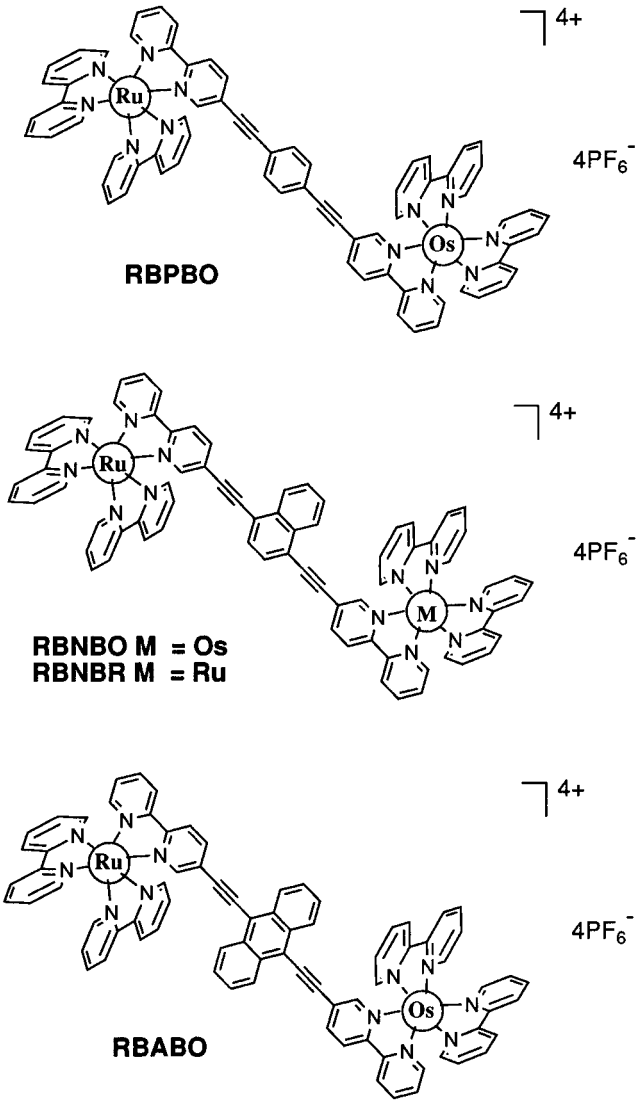

the mononuclear complexes (e.g., **RBP**) used as reference materials. The counteranion is hexafluorophosphate in each case. The polytopic ligands are identified by their three constituent units (e.g., **BPB**).

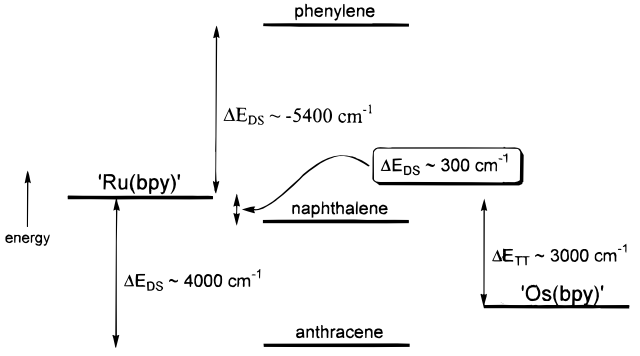

Figure 1. Pictorial representation of the relative triplet energy levels for the Ru(bpy) and Os(bpy) terminals and for the connecting spacer fragment. Quoted values refer to the corresponding mononuclear complexes or the free ligands and were measured by luminescence spectroscopy.

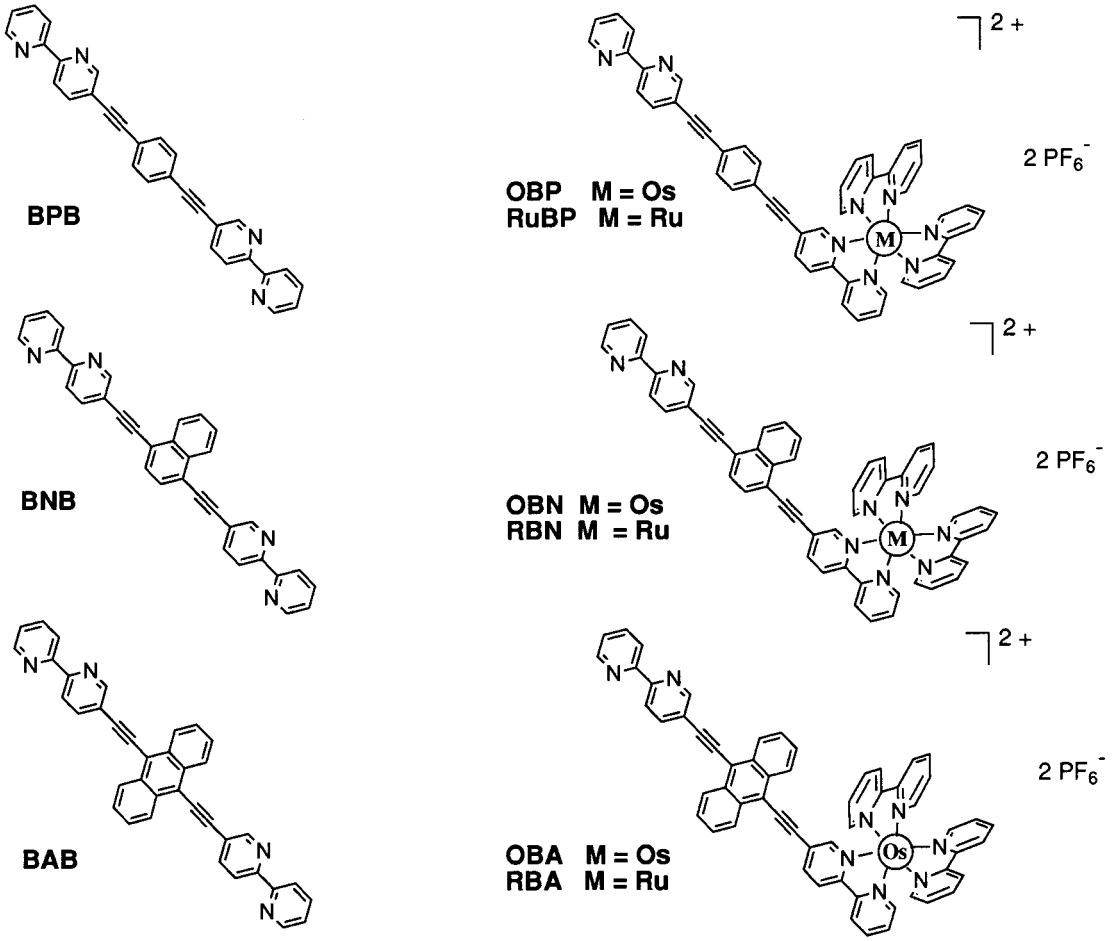

The mixed-metal triads have their metal centers separated by ca. 18 Å and share a common geometry.[16] Photophysical properties have been recorded for the various mono- and binuclear Ru and Os complexes and, throughout the present investigation, we refer to the mononuclear complexes as reference compounds.[23] These earlier studies located triplet energy levels for each molecular fragment and the general situation is depicted in Figure 1 with the values being compiled in Table 1. Thus, triplet energies of the various metal complexes show a slight dependence on the nature of the connector but the triplet energy of the Ru(bpy) terminal invariably exceeds that of the appended Os(bpy) unit by a substantial amount. Table 1 lists these spectroscopic energy gaps (ΔE_{TT}) calculated from luminescence spectra recorded[23] for the mononuclear reference compounds in acetonitrile at 20 °C. The triplet state localized on the phenylene-based connector **BPB** lies at much higher energy than the triplets associated with either terminal. This situation is quantified by the energy gap (ΔE_{DS}) between triplets localized on a terminal metal complex and on the connector (Table 1); note, a negative ΔE_{DS} indicates that the triplet localized on the connector lies at higher energy than the corresponding triplet associated with the metal complex terminal. The triplet state localized on the naphthalene-based connector **BNB** is at slightly lower energy than that associated with the Ru(bpy) fragment but greatly exceeds the triplet energy of the Os(bpy) terminal. This case is particularly interesting because the energy of the connector triplet lies between those of the terminals while the small ΔE_{DS} should promote reversible triplet energy transfer between the Ru(bpy) terminal and the connector. The triplet energy of the anthracene-based connector **BAB** is lower than those of the terminals but lies fairly close to the triplet associated with the Os(bpy) fragment (Table 1). The

TABLE 1: Spectroscopic Properties Recorded for the Various Mononuclear Reference Compounds or Free Ditopic Ligands

property	RBP	RBN	RBA	OBP	OBN	OBA	RBPBO	RBNBO	RBABO
E_T (Ru)/cm^{-1}[a]	16570	16405	16300	13575	13385	13150			
ΔE_{TT}/cm^{-1}[b]							2995	3020	3150
ΔE_{DS}/cm^{-1}[c]	−5400	305	3900	−8395	−2715	750			
Φ_L[d]	0.056	0.035	<0.001	0.0014	0.0014	0.0021			
λ_L/nm[e]	650	656	670	790	800	800			
λ_T/cm^{-1}[f]							2285	2075	2200
τ_T/ns[g]	980	7500	0.082	22	18	415			
$J_F/10^{-14}$ mmol^{-1} cm^6							2.8	2.8	3.0
$J_D/10^{-4}$ cm							1.9	1.9	2.0
k_F/μs^{-1}[h]							8.4	8.5	8.7

[a] Triplet energy of the terminal metal complex at 20 °C. [b] Difference in triplet energy between the Ru(bpy) and Os(bpy) terminals. [c] Difference in energy between triplet states localized on a metal complex terminal and on the connecting polytopic ligand. [d] Emission quantum yield. [e] Luminescence maximum. [f] Total re-organization energy accompanying triplet energy transfer. [g] Triplet lifetime in deoxygenated acetonitrile. [h] Overall rate constant for Förster-type intramolecular triplet energy transfer between the terminals.

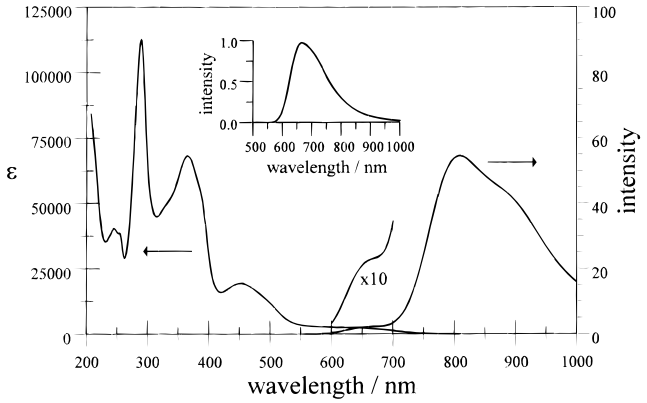

Figure 2. Absorption and luminescence spectra recorded for **RBPBO** in deoxygenated acetonitrile solution at 20 °C. The excitation wavelength for the emission spectrum was 460 nm while the region where luminescence from the Ru(bpy) fragment is expected to be predominant is shown on a 10× expanded scale. The insert shows the emission spectrum recorded under identical conditions for an equimolar mixture of **RBP** and **OBP**.

energy gap between these latter triplets ($\Delta E_{DS} = 750$ cm^{-1}) is sufficiently small so as to facilitate reversible triplet energy transfer in the reference compound **OBA**.[30]

Long-Range Energy Transfer in RBPBO. The absorption spectrum recorded for **RBPBO** shows a low-intensity tail stretching across the far-red region of the spectrum that can be ascribed to the spin-forbidden, metal-to-ligand, charge-transfer transition associated with the Os(bpy) fragment[31] (Figure 2). Excitation into this band ($\lambda = 648$ nm) produces emission from the Os(bpy) unit which decays via exponential kinetics corresponding to a triplet lifetime (τ_T) of 25 ± 3 ns, as measured at 800 nm. This latter value is close to that recorded ($\tau_T = 22 \pm 2$ ns) for the reference compound **OBP** in deoxygenated acetonitrile[23] while identical emission quantum yields ($\Phi_L = 0.0014$) are found for these two compounds. After deconvolution of the instrument response function, it is clear that the emitting species is formed within the temporal resolution of the instrument (i.e., 200 ps), as might be expected for direct illumination into the emitting chromophore (Figure 3a). In contrast, when excitation of **RBPBO** is made at 460 nm, where the two terminals compete almost equally for incident photons, decay profiles recorded between 750 and 850 nm show that a significant portion (i.e., 20−40%) of the total luminescence signal grows-in after the laser pulse (Figure 3b). This behavior is indicative of intramolecular triplet energy transfer along the molecular axis, and is supported by the observation that the corrected excitation spectrum closely matches the absorption spectrum over the entire visible region. The rate constant for this process, measured by global analysis methodology after deconvolution of the instrument response function, is $8 \pm 1 \times 10^8$ s^{-1}.

Examination of the emission spectrum of **RBPBO** in the region where the Ru(bpy) fragment is expected to emit most strongly ($630 < \lambda < 680$ nm) but where the Os(bpy) unit does not emit shows the presence of residual luminescence from the Ru(bpy) chromophore (Figure 2). When compared to the luminescence spectrum recorded for an optically matched equimolar mixture of **RBP** and **OBP**, it is seen that emission from the Ru(bpy) fragment in **RBPBO** is quenched by >99%. The luminescence lifetime recorded at 650 nm, this being close to the emission maximum of the Ru(bpy) fragment (Table 1), after excitation at 460 nm is 1.25 ± 0.08 ns (Figure 3c). Under identical conditions, the emission lifetime of the Ru(bpy)

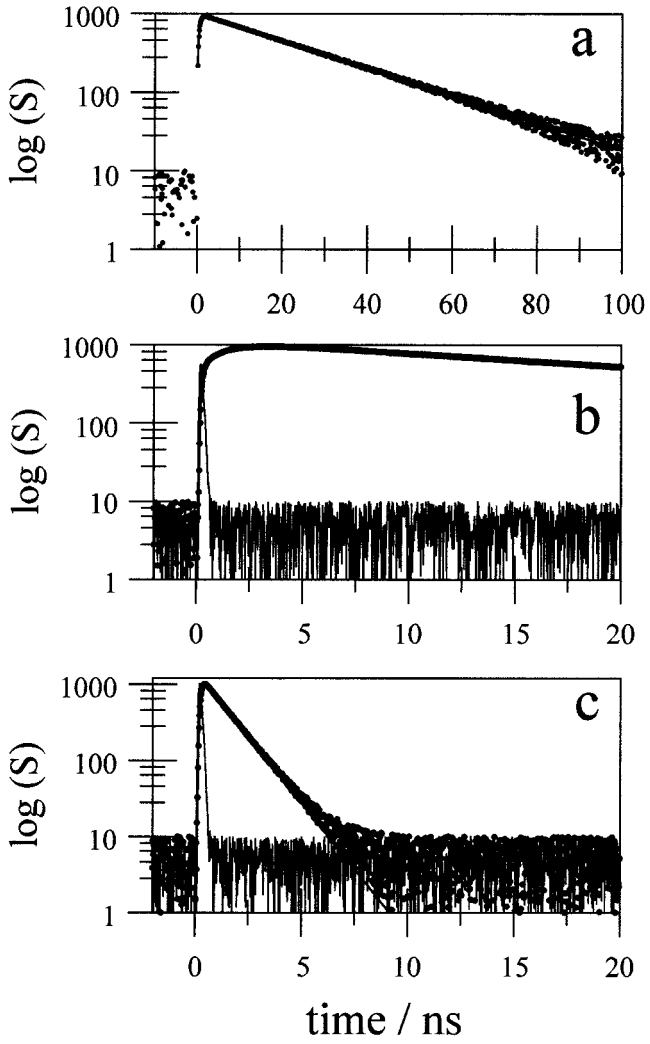

Figure 3. Time-resolved luminescence decay profiles recorded for **RBPBO** in deoxygenated acetonitrile at 20 °C under the following conditions: (a) excitation at 648 nm with detection at 800 ± 10 nm, (b) excitation at 460 nm with detection at 800 ± 10 nm, and (c) excitation at 460 nm with detection at 650 ± 2 nm. The instrumental response function is shown as a solid line on traces (b) and (c). In each case, the excitation source was a 25 ps laser pulse delivered from a mode-locked Nd:YAG laser equipped with a Raman shifter and detection was by a fast-response photodiode.

chromophore in the equimolar mixture is 900 ± 25 ns. The overall quenching rate constant (k_{ET}), calculated as the difference between triplet lifetimes recorded for the Ru(bpy) fragments in **RBPBO** and **RBP**, can now be confirmed as being $8 \pm 1 \times 10^8$ s^{-1}.

Triplet energy transfer is to be expected in this system since the triplet state localized on the Os(bpy) fragment lies about 3000 cm^{-1} below that of the Ru(bpy) triplet while the total reorganization energy (λ_T) accompanying energy transfer is 2285 cm^{-1} (Table 1).[16] The large energy gap ($\Delta E_{TT} \approx 13 k_B T$), taken together with the relatively short lifetime found for the Os(bpy) triplet, does not facilitate reverse energy transfer but ensures that k_{ET} will be close to the apex of a Marcus rate vs energy gap profile since $\Delta E_{TT} \approx \lambda_T$.[32] Furthermore, the triplet state localized on the connecting phenylene residue is known[23] to lie at much higher energy than that of the Ru(bpy) donor so that it is unlikely to be populated as a real intermediate during energy transfer. In agreement with many other studies,[2,12,33] therefore, it appears that long-range, intramolecular triplet energy transfer occurs in **RBPBO**. The rate of energy transfer is several

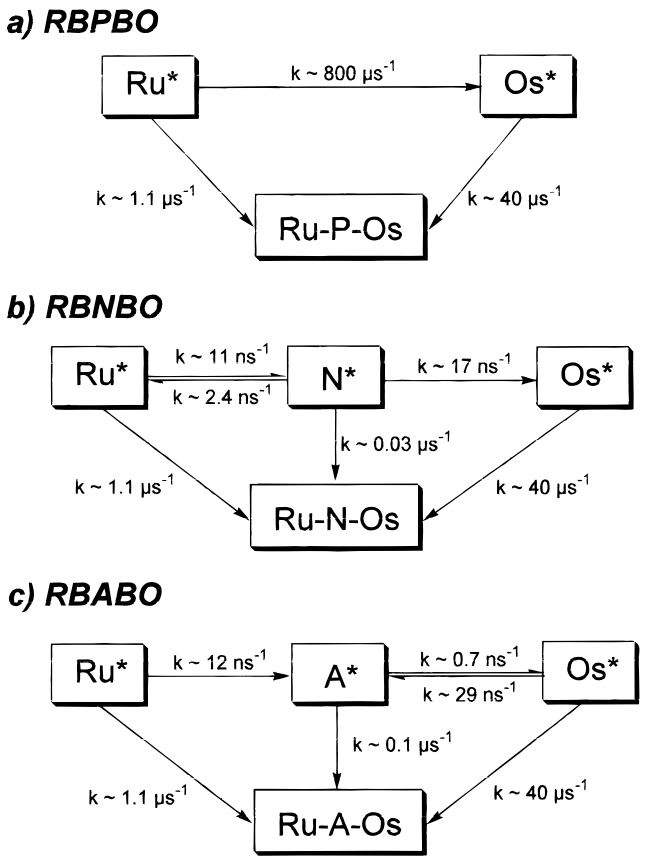

Figure 4. Compartmental kinetic models indicating the course of intramolecular triplet energy transfer and competing deactivation in the various molecular triads. Kinetic data refer to either the triad or the corresponding mononuclear complexes in deoxygenated acetonitrile at 20 °C with excitation into one of the terminal metal complexes.

TABLE 2: Parameters Relating to Intramolecular Electron Exchange in the Molecular Triads at 20 °C

compound	process[a]	$k_{ET}/10^8$ s^{-1}	FC/10^{-4} cm	V_{DA}/cm^{-1}
RBPBO	Ru* → Os	8.0	1.9	1.9
RBNBO	Ru* → NAP	110	0.66	11.7
	NAP* → Ru	24	0.15	11.5
	NAP* → Os	170	1.8	8.9
RBABO	Ru* → ANT	120	1.9	7.3
	Os* → ANT	290	1.7	11.8
	ANT* → Os	7.2	0.044	11.6

[a] The particular process under consideration refers either to long-range triplet energy transfer between the terminals (e.g., Ru* → Os) or between one of the terminals and the corresponding connector (where NAP* and ANT*, respectively, refer to the naphthalene-like and anthracene-like triplets).

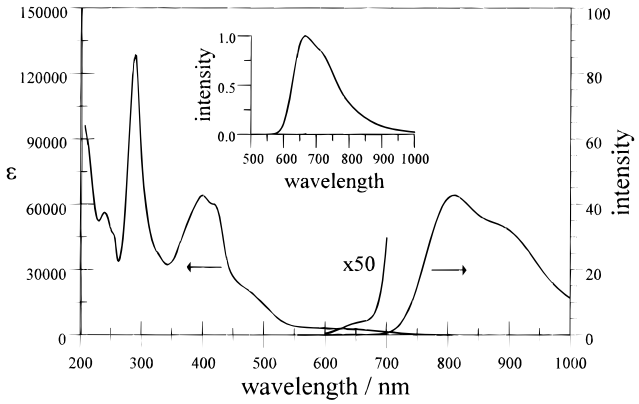

Figure 5. Absorption and luminescence spectra recorded for **RBNBO** in deoxygenated acetonitrile solution at 20 °C. The excitation wavelength for the emission spectrum was 490 nm while the region where luminescence from the Ru(bpy) fragment is expected to be predominant is shown on a 50× expanded scale. The insert shows the emission spectrum recorded under identical conditions for an equimolar mixture of **RBN** and **OBN**.

orders of magnitude slower than found for the corresponding ethynylene-bridged system ($k_{ET} = 2.5 \times 10^{11}$ s^{-1})[12] but is comparable to that reported recently ($k_{ET} = 6.7 \times 10^8$ s^{-1}) for a system having the Ru(bpy) and Os(bpy) terminals separated by three phenylene rings.[33] This crude comparison suggests that each ethynylene group operates as a phenylene ring although, of course, the actual situation is much more complicated.

Unidirectional compartmental triplet energy transfer, therefore, can be considered to take place between the terminals according to Figure 4a. The initially formed Ru(bpy) triplet decays exponentially, with a lifetime of 1.25 ns, to form the corresponding triplet localized on the Os(bpy) fragment. Long-range energy transfer is almost quantitative in this system, assisted by the long inherent lifetime of the donor, although the acceptor triplet is relatively short-lived and the full yield is not attained because of competitive deactivation. The transfer process is considered to involve both Förster dipole−dipole[34] and Dexter electron-exchange[3,4] mechanisms, but their relative contributions can be estimated from consideration of appropriate spectral overlap integrals.[35,36] Evaluation of these integrals is easily made by reference to absorption and emission spectra recorded, respectively, for **OBP** and **RBP** in acetonitrile. Thus, spectral overlap integrals for Förster ($J_F = 2.8 \times 10^{-14}$ cm^6 mmol^{-1}) and Dexter ($J_D = 1.9 \times 10^{-4}$ cm) processes remain comparable to those determined for related metal complexes.[37,38] Using photophysical properties measured for **RBP**,[23,16] the rate constant for dipole−dipole energy transfer in **RBPBO** is calculated to be ca. 8.4×10^6 s^{-1}, which is ca. 1% of the measured rate of energy transfer. Consequently, triplet energy transfer is considered to take place via electron exchange, despite the insulating role played by the central phenylene residue, so that the electronic coupling matrix element (V_{DA}) can be estimated[35,36] from eq 1 as being ca. 2 cm^{-1} (Table 2).

$$k_{ET} = \frac{2\pi}{\hbar}|V_{DA}|^2 J_D \qquad (1)$$

I**ndirect Energy Transfer in RBNBO**. The naphthalene-based ditopic ligand in **RBNBO** absorbs strongly between 350 and 450 nm,[23,30] but the spin-allowed MLCT transitions associated with the two metal complexes appear as a pronounced shoulder centered around 500 nm (Figure 5). Excitation of **RBNBO** in deoxygenated acetonitrile at 648 nm, where only the Os(bpy) unit absorbs, results in luminescence from that fragment which decays via exponential kinetics ($\tau_T = 20 \pm 3$ ns) and for which the quantum yield is 0.0015. Both values remain close to those measured previously[23] for **OBN** (Table 1). The corrected excitation spectrum is in good agreement with the absorption spectrum recorded over the entire visible region, including where the multitopic ligand absorbs strongly. Luminescence from the Ru(bpy) unit, which dominates the emission profile recorded for an equimolar mixture of **RBN** and **OBN** with excitation at 490 nm, makes only a very minor contribution to the emission spectrum recorded for the triad under identical conditions (Figure 5).

It was established earlier[23] that triplet states localized on Ru(bpy) and on the naphthalene-based connector are in thermal equilibrium ($\Delta E_{DS} \approx k_B T$) for **RBN**, the equilibrium mixture

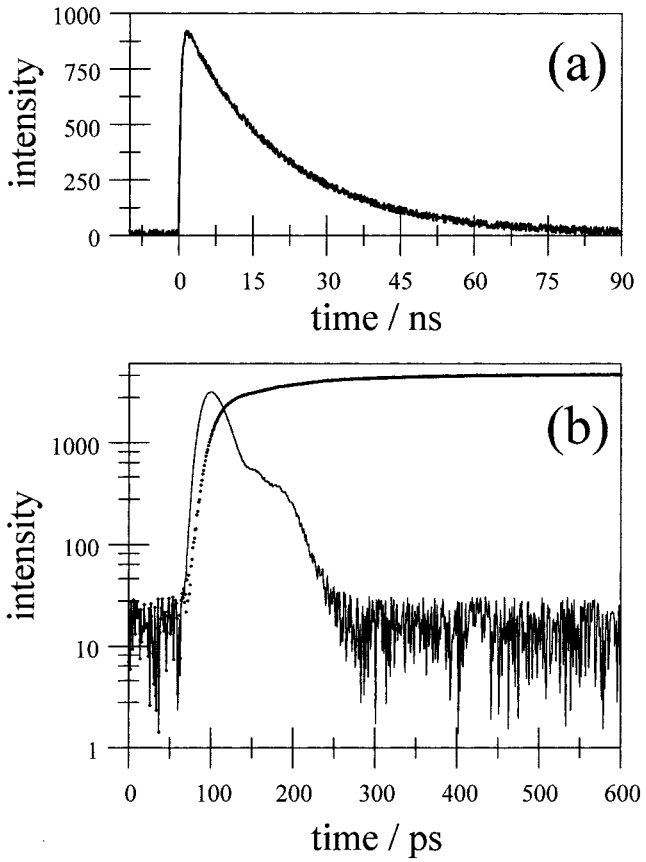

Figure 6. Time-resolved luminescence decay profiles recorded at 800 ± 10 nm following excitation of **RBNBO** in deoxygenated acetonitrile at 20 °C with a 6 ps laser pulse at 532 nm. Decay curve measured with (a) a fast-response photodiode and (b) the streak camera. The instrumental response function is shown on trace (b) as a solid line.

decaying via first-order kinetics with a lifetime of 7.5 μs. The very low luminescence yield implicated for the Ru(bpy) fragment in **RBNBO**, relative to **RBN** and **RBNBR**, suggests that this equilibrium mixture of triplet states decays much faster for the triad than for the corresponding diad. The most likely reason for such behavior is that intramolecular energy transfer from the connector triplet to the terminal Os(bpy) fragment competes with deactivation of the equilibrium mixture of triplet states. In fact, monitoring emission from the Os(bpy) unit following laser excitation at 532 nm, where the Ru(bpy) fragment absorbs ca. 40% of incident photons, shows that the emitting species are formed in two kinetically distinct steps (Figure 6). Most (i.e., ca. 70%) of the emitting species are formed within the excitation pulse and decay with a lifetime of 20 ± 2 ns. About 30% of the emitting species, however, are formed after the excitation pulse while retaining the same spectral profile and decay kinetics as observed for those triplets produced by direct excitation into the Os(bpy) fragment. Formation of the emitting Os(bpy) triplet is complete within about 500 ps but the kinetics appear to be complex and it has not been possible to derive an accurate rate constant for this secondary growth.

Luminescence decay curves recorded at 650 nm, where the Ru(bpy) triplet is expected to be the sole emitting species, following excitation at 532 nm correspond to the sum of two exponentials (Figure 7). Combining data collected over different time regimes indicates that the two lifetimes are $\tau_1 = (45 \pm 7)$ and $\tau_2 = (120 \pm 20)$ ps while their respective fractional amplitudes at 650 nm are $A_1 = 19\%$ and $A_2 = 81\%$. These lifetimes should be compared with those recorded[23] for **RBN**

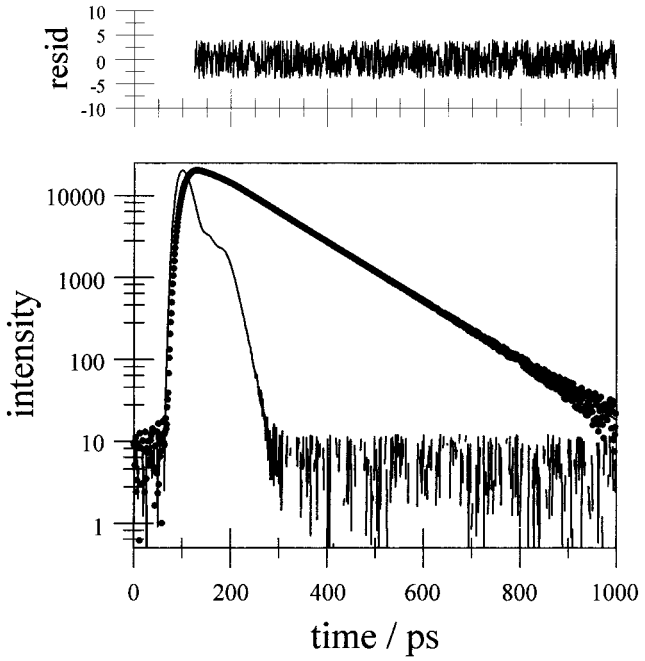

Figure 7. Time-resolved luminescence decay profile recorded at 650 ± 2 nm following excitation of **RBNBO** in deoxygenated acetonitrile at 20 °C with a 6 ps laser pulse at 532 nm. The instrumental response function is shown as a solid line, while the weighted residuals are shown above the experimental record. The data are fit to a two-exponental decay law, as explained in the text.

under similar conditions where the Ru(bpy) triplet also decays by way of dual-exponential kinetics but with lifetimes of 75 ps and 7.5 μs. The triplet state properties recorded[16] for the symmetric binuclear complex **RBNBR** remain very similar to those recorded for **RBN** so that it is the presence of the terminal Os(bpy) complex that shortens τ_2 in **RBNBO**.

The results can now be discussed in terms of the intercompartmental triplet energy transfer scheme outlined in Figure 4b. Here, the triplet state localized on the Os(bpy) terminal retains a lifetime of 20 ns, regardless of how it is populated, and does not enter into intramolecular energy transfer with other components of the system. The triplet state localized on the Ru(bpy) terminal transfers energy to the naphthalene-based connector but, because of the small energy gap ($\Delta E_{TT} = 305$ cm^{-1}), this process is reversible.[16,23] The energy gap corresponds to an equilibrium constant of 4.5 and implies that the equilibrium mixture will comprise ca. 20% of the triplet localized on the Ru(bpy) terminal. Using rate constants for the forward ($k_{ET} = 10.9$ ns^{-1}) and reverse ($k_{ET} = 2.4$ ns^{-1}) energy-transfer processes measured[23] for **RBN** together with the derived triplet lifetimes of 45 and 120 ps it can be shown[39,40] that the rate constant for energy transfer from the connector triplet to the Os(bpy) terminal must have a value of ca. 1.7×10^{10} s^{-1}. This rate ensures that triplet energy transfer along the molecular axis is essentially quantitative.

Each of the three energy-transfer steps is considered to take place via the Dexter-type electron-exchange mechanism[3,4] since Förster overlap integrals for the individual steps are negligible. It is not possible to estimate Dexter-type overlap integrals for these processes but all the necessary spectroscopic information exists by which to calculate[29,36] Franck−Condon (FC) factors for each electron-exchange step (Table 2). These FC factors can be used as replacements[36] for the J_D term in eq 1 so that the corresponding electronic coupling matrix elements V_{DA} for electron exchange can be estimated (Table 2). The derived values suggest that electronic coupling between Ru(bpy) and

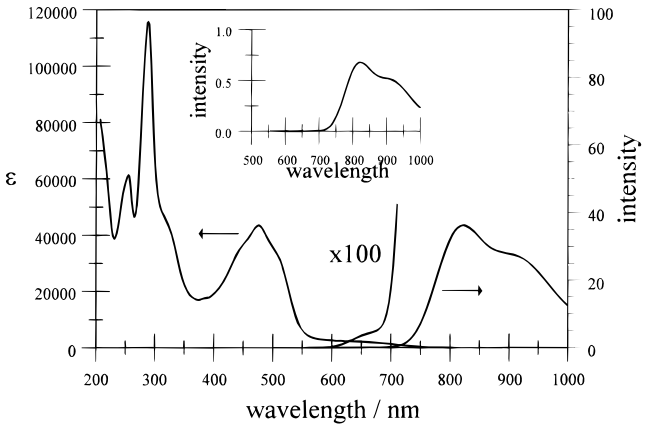

Figure 8. Absorption and luminescence spectra recorded for **RBABO** in deoxygenated acetonitrile solution. The excitation wavelength for the emission spectrum was 540 nm while the region where luminescence from the Ru(bpy) fragment is expected to be significant is shown on a 100× expanded scale. The insert shows the emission spectrum recorded under identical conditions for an equimolar mixture of **RBA** and **OBA**.

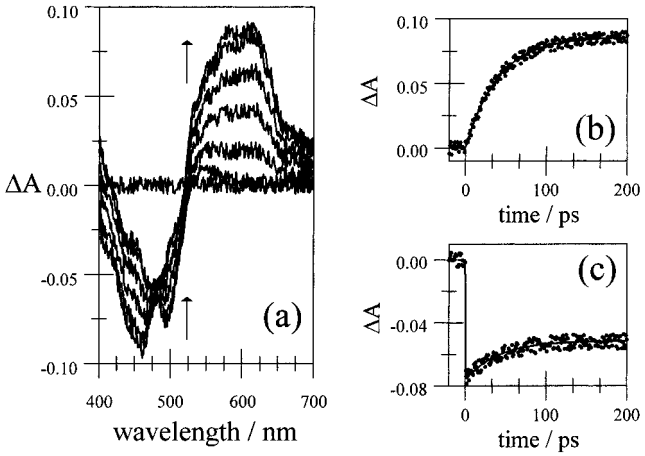

Figure 9. (a) Differential transient absorption spectra recorded after excitation of **RBABO** in deoxygenated acetonitrile with a subpicosecond laser pulse at 600 nm. Individual spectra were recorded before the laser pulse and at delay times of 5, 10, 20, 50, 100, and 200 ps. Traces (b) and (c), respectively, show decay profiles recorded at 600 and 490 nm.

the connector is slightly stronger than between the connector and Os(bpy), although all the values remain in the same range. The results also indicate that long-range Förster energy transfer between the terminals does not compete with two-step electron exchange in this system (Table 1).

Energy Leakage in RBABO. Detailed investigation of the energy-transfer processes occurring in **RBABO** is rendered difficult by the absorption profile of the multitopic ligand,[30] which extends over the range 300−520 nm and masks MLCT bands associated with the terminals (Figure 8). In particular, it is not possible to isolate a wavelength range over which the Ru(bpy) fragment is the dominant chromophore. Furthermore, luminescence from the equimolar mixture of reference compounds **RBA** and **OBA** is dominated by emission from the Os(bpy) unit[16,30] to such an extent that emission from the Ru(bpy) fragment cannot be properly resolved from the baseline (Figure 8). Previous work[23] has established that intramolecular triplet energy transfer from the Ru(bpy) unit to the anthracene-based connector is extremely efficient in **RBA** ($k_{ET} = 12$ ns^{-1}, $\Delta E_{TT} = 3900$ cm^{-1}) and there is no reason to suppose that the same process does not take place in **RBABO**. As with the equimolar mixture of reference compounds, excitation of **RBABO** in deoxygenated acetonitrile at 540 nm, where the Ru(bpy) fragment absorbs ca. 40% of incident photons, gives rise to an emission spectrum characteristic of the Os(bpy) fragment without obvious contamination by emission from the Ru(bpy) unit (Figure 8). By itself, this observation is not to be taken as evidence for triplet energy transfer along the molecular axis since the Os(bpy) fragment absorbs ca. 60% of incident photons at 540 nm.

Excitation of **RBABO** in deoxygenated acetonitrile at 648 nm, where the Os(bpy) unit is the sole chromophore, gives rise to relatively strong ($\Phi_L = 0.0012$) emission characteristic of the Os(bpy) unit. The emission lifetime ($\tau_T = 345 \pm 15$ ns) is surprisingly long. Excitation of the sample with a subpicosecond laser pulse at 600 nm shows that the initially formed Os(bpy) triplet converts to the anthracene-like triplet with a first-order rate constant of $(3.0 \pm 0.5) \times 10^{10}$ s^{-1} (Figure 9). These observations, being similar to those made earlier with **OBA**,[30] are consistent with rapid triplet energy transfer from Os(bpy) to the anthracene-based connector so as to establish an equilibrium mixture of triplet states in which the Os(bpy) triplet is reformed via slower reverse energy transfer. The triplet energy gap ($\Delta E_{TT} \approx 750$ cm^{-1}), while strongly favoring the anthracene-like triplet, is sufficiently small to allow reverse energy transfer to compete with inherent deactivation of the anthracene-like triplet. The equilibrium constant calculated from the spectroscopic energy gap is 40 so that the fraction of Os(bpy) triplets in the equilibrium mixture is only ca. 2.5%. This fraction is too small to perturb the transient absorption spectrum, which closely resembles that recorded for **BAB**,[23] but is sufficient for easy detection by luminescence spectroscopy since the anthracene-like triplet does not emit under these conditions.

To a first approximation, the two terminals present in **RBABO** appear to act independently and both transfer triplet energy to the connector. Transient absorption spectra recorded after excitation of **RBABO** with a 10 ns laser pulse at 532 nm are very similar to that recorded for the ditopic ligand **BAB**.[23] This confirms that the triplet localized on the connector lies at lower energy than the triplets of either terminal. The corrected excitation spectrum recorded by monitoring emission from the Os(bpy) fragment agrees well with the absorption spectrum recorded over the entire visible region, even where the Ru(bpy) unit absorbs strongly. These various findings can be accommodated within the compartmental model displayed in Figure 4c where slow triplet energy leakage occurs from the connector to the Os(bpy) terminal. It is interesting to note that, according to the derived V_{DA} values (Table 2), the Ru(bpy) triplet appears to be somewhat less well coupled to the connector than is the Os(bpy) triplet. This is the opposite situation to that found for the corresponding naphthalene-based system, suggesting that the nature of the connector exerts a marked influence on coupling to individual subunits that is not easily explained at present.

Comparison of the Three Connectors. The three molecular systems can be compared in terms of a computer simulation of the energy-transfer processes expected to occur following selective excitation into the Ru(bpy) fragment. This situation cannot be realized experimentally, but the necessary kinetic information is available to solve the various differential equations associated with the compartmental models illustrated in Figure 4. In fact, the idealized situation is almost attainable for **RBPBO** so that little speculation is involved in the simulation. For both **RBNBO** and **RBABO**, however, the models rely heavily on data collected for the mononuclear reference compounds.

Long-range triplet energy transfer in **RBPBO** involves only two intermediate species and with the connector mediating the

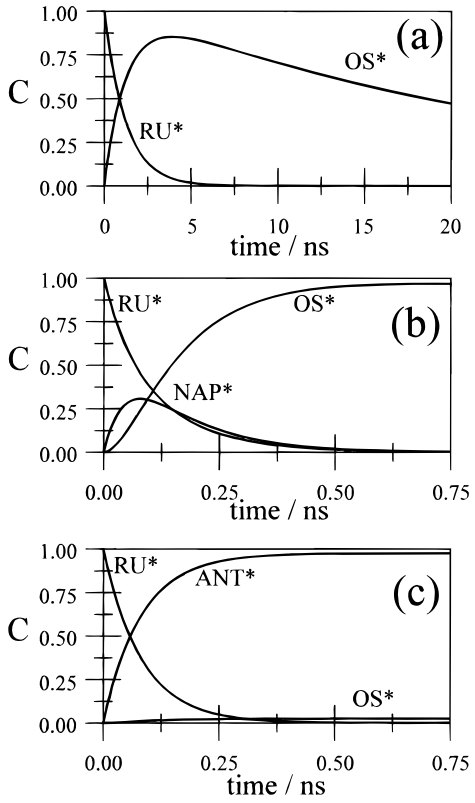

Figure 10. Simulated concentration (C) profiles showing the expected course of reaction following immediate and selective population of the triplet state localized on the Ru(bpy) fragment of the various triads. Profiles refer to (a) **RBPBO**, (b) **RBNBO**, and (c) **RBABO** while kinetic data are taken from Figure 4. The notations are explained as follows: RU* and OS* refer, respectively, to triplets localized on Ru(bpy) and Os(bpy) terminals, NAP* is the triplet localized on the naphthalene-like connector, and ANT* is the triplet state localized on the anthracene-like connector.

process via superexchange. The rate of intramolecular energy transfer is not that much faster than the inherent rate of deactivation of the Os(bpy) acceptor such that the maximum attainable yield of Os(bpy) triplet is restricted to ca. 85% (Figure 10). Electronic coupling between the terminals ($V_{DA} = 2$ cm^{-1}) is kept modest by the large separation and by the poor connectivity between ethynylene and phenylene units. Furthermore, the large energy gap ($\Delta E_{DS} = -5400$ cm^{-1}) between triplet states localized on donor and connector units is not conducive for fast long-range energy transfer between the terminals since it limits electronic coupling occurring via superexchange interactions.[41] Since the connector triplet is not populated as a real intermediate, this system operates as a diad not a triad. Numerous related systems have been described in the literature.[2,12,33]

Three intermediate species are needed to properly model the energy-transfer processes taking place in **RBNBO** (Figure 10). Initial population of the Ru(bpy) triplet leads to rapid establishment of an equilibrium with the connector triplet, such that the Ru(bpy) triplet decays via dual-exponential kinetics. In the reference compound **RBN** this equilibrium mixture survives for ca. 8 μs,[23] but it is quickly dissipated in **RBNBO** because of energy transfer from the connector triplet to the Os(bpy) terminal. Thus, formation of the Os(bpy) triplet is complete within 700 ps, the maximum attainable yield being ca. 97%, and this appears as an important increase in rate compared to **RBPBO**. Within the confines of the two-step mechanism, the concentration of the intermediate connector triplet never surpasses ca. 30% of the total triplet population but this species plays a critical role in the overall process. Each step is believed to involve electron exchange without competition from dipole−dipole interactions. As such, electronic coupling between Ru(bpy) and the connector is somewhat more pronounced than between the connector and Os(bpy) but the two-step process shows a clear increase in electronic coupling compared to the long-range transfer deduced for **RBPBO**.

Selective excitation of the Ru(bpy) fragment in **RBABO** is expected to be followed by rapid triplet energy transfer to the connector, as has been demonstrated for **RBA**.[23] The concentration of triplet Ru(bpy) quickly falls to zero while the connector triplet accumulates (Figure 10). This latter species is not a relay in the usual sense[15,16] but is coupled to the terminal Os(bpy) unit by way of reversible energy transfer. As such, an equilibrium mixture of triplets is established in which the Os(bpy) fragment contributes only 2.5%, the remainder being provided by the connector. The advantage of this system is that the triplet lifetime of the Os(bpy) unit is greatly prolonged since the equilibrium mixture decays with a common lifetime of 345 ns. Leakage of triplet energy along the molecular axis, therefore, provides a useful alternative to both long-range and indirect energy transfer.

Acknowledgment. We thank the C.N.R.S., and the E.C.P.M. for their financial support of this work. We are greatly endebted to Johnson-Matthey Ltd. for their generous loan of precious metal salts.

Supporting Information Available: Supporting information provides a description of the methodology used to derive rate constants for electron exchange in each of the multicomponent systems. This material is available free of charge via the Internet at http://pubs.acs.org.

References and Notes

(1) For leading references see: (a) Harriman, A. *R.S.C. Spec. Period. Rep.*: *Photochemistry* **2000**, *30*, 1. (b) Guldi, D. M.; Torres-Garcia, G.; Mattay, J. *J. Phys. Chem. A* **1998**, *102*, 9679. (c) Högemann, C.; Vauthey, E. *J. Phys. Chem. A* **1998**, *102*, 10051.

(2) For leading references see: (a) Barigelletti, F.; Flamigni, L. *Chem. Soc. Rev.* **2000**, *29*, 1. (b) Scwab, P. F. H.; Levin, M. D.; Michl, J. *Chem. Rev.* **1999**, *99*, 1863. (c) Balzani, V.; Juris, A.; Venturi, M.; Campagna, S.; Serroni, S. *Chem. Rev.* **1996**, *96*, 750.

(3) Dexter, D. L. *J. Chem. Phys.* **1953**, *21*, 836.

(4) (a) Sigman, M. E.; Closs, G. L. *J. Phys. Chem.* **1991**, *95*, 5012. (b) MacQueen, D. B.; Eyler, J. R.; Schanze, K. S. *J. Am. Chem. Soc.* **1992**, *114*, 1997.

(5) Reimers, J. R.; Hush, N. S. *J. Phys. Chem. A* **1999**, *103*, 3066, and references therein.

(6) Harriman, A.; Romero, F. M.; Ziessel, R.; Benniston, A. C. *J. Phys. Chem. A* **1999**, *103*, 5399.

(7) Harriman, A.; Hissler, M.; Jost, P.; Wippf, G.; Ziessel, R. *J. Am. Chem. Soc.* **1999**, *121*, 14.

(8) Ford, W. E.; Rodgers, M. A. J. *J. Phys. Chem.* **1992**, *96*, 2917.

(9) (a) Wilson, G. J.; Sasse, W. H. F.; Mau, A. W.-H. *Chem. Phys. Lett.* **1996**, *250*, 583. (b) Wilson, G. J.; Launikonis, A.; Sasse, W. H. F.; Mau, A. W.-H. *J. Phys. Chem.* **1997**, *101*, 4860.

(10) Harriman, A.; Hissler, M.; Khatyr, A.; Ziessel, R. *Chem. Commun.* **1999**, 735.

(11) Hissler M.; Harriman, A.; Khatyr, A.; Ziessel, R. *Chem.: Eur. J.* **1999**, *5*, 3366.

(12) (a) Grosshenny, V.; Harriman, A.; Ziessel, R. *Angew. Chem., Int. Ed. Engl.* **1995**, *34*, 2705. (b) Benniston, A. C.; Harriman, A.; Grosshenny, V.; Ziessel, R. *New J. Chem.* **1997**, *21*, 405. (c) Harriman, A.; Hissler, M.; Ziessel, R.; De Cian, A.; Fischer, J. *J. Chem. Soc., Dalton Trans.* **1995**, 4067.

(13) Samanta, M. P.; Tian, W.; Datta, S.; Hendersen, J. L.; Kubiak, C. P. *Phys. Rev. B*: *Condens. Matter* **1996**, *53*, 7626.

(14) Benniston, A. C.; Grosshenny, V.; Harriman, A.; Ziessel, R. *Angew. Chem., Int. Ed. Engl.* **1994**, *33*, 1884.

(15) Belser, P.; Dux, R.; Baak, M.; De Cola, L.; Balzani, V. *Angew. Chem., Int. Ed. Engl.* **1995**, *34*, 595.

(16) El-ghayoury, A.; Harriman, A.; Khatyr, A.; Ziessel, R. *Angew. Chem., Int. Ed*., in press.
(17) Sessler, J. L.; Capuano, V. L.; Harriman, A. *J. Am. Chem. Soc*. **1993**, *115*, 4618.
(18) (a) Strachen, J.-P.; Gentemann, S.; Seth, J.; Kalsbeck, W. A.; Lindsey, J. S.; Holten, D.; Bocian, D. F. *J. Am. Chem. Soc*. **1997**, *119*, 11191. (b) Li, F.; Gentemann, S.; Kalsbeck, W. A.; Seth, J.; Lindsey, J. S.; Holten, D.; Bocian, D. F. *J. Mater. Chem*. **1997**, *7*, 1245. (c) Van Patten, P. G.; Shreve, A. P.; Lindsey, J. S.; Donohue, R. J. *J. Phys. Chem. B* **1998**, *102*, 4209.
(19) (a) Strouse, G. F.; Worl, L. A.; Younathan, J. N.; Meyer, T. J. *J. Am. Chem. Soc*. **1989**, *111*, 9101. (b) Jones, W. E.; Baxter, S. M.; Meckleberg, S. L.; Erickson, B. W.; Peek, B. M.; Meyer, T. J. In *Supramolecular Chemistry*; Balzani, V., De Cola, L., Eds.; Kluwer: Dordrecht, 1992; p 248.
(20) (a) Harriman, A.; Ziessel, R. *Chem. Commun*. **1996**, 1717. (b) Harriman, A.; Ziessel, R. *Coord. Chem. Rev*. **1998**, *171*, 331.
(21) El-ghayoury, A.; Harriman, A.; Hissler, M.; Ziessel, R. *Coord. Chem. Rev*. **1998**, *178*−*180*, 1251.
(22) El-ghayoury, A.; Ziessel, R. *Tetrahedron Lett*. **1997**, *38*, 2471.
(23) El-ghayoury, A.; Harriman, A.; Khatyr, A.; Ziessel, R. *J. Phys. Chem. A* **1999**, *103*, 5399.
(24) Sprintschnik, G.; Sprintschnik, H. W.; Kirsch, P. P.; Whitten, D. *J. Am. Chem. Soc*. **1977**, *99*, 4947.
(25) Grosshenny, V.; Romero, F. M.; Ziessel, R. *J. Org. Chem*. **1997**, *62*, 1491.
(26) Caspar, J. V.; Kober, E. M.; Sullivan, B. P.; Meyer, T. J. *J. Am. Chem. Soc*. **1982**, *104*, 630.
(27) Kober, E. M.; Marshall, J. L.; Dressick, W. J.; Sullivan, B. P.; Caspar, J. V.; Meyer, T. J. *Inorg. Chem*. **1985**, *24*, 2755.
(28) Lami, H.; Piermont, T. *Chem. Phys*. **1992**, *163*, 149.
(29) (a) Murtaza, Z.; Zipp, A. P.; Worl, L. A.; Graff, D. K.; Jones, W. E., Jr.; Bates, W. D.; Meyer, T. J. *J. Am. Chem. Soc*. **1991**, *113*, 5113. (b) Murtaza, Z.; Graff, D. K.; Zipp, A. P.; Worl, L. A.; Jones, W. E., Jr.; Bates, W. D.; Meyer, T. J. *J. Phys. Chem*. **1994**, *98*, 10504. (c) Ryu, C. K.; Schmehl, R. H. *J. Phys. Chem*. **1989**, *93*, 7961. (d) Katayama, H.; Maruyama, S.; Ito, S.; Tsuji, Y.; Tsuchida, A.; Yamamoto, M. *J. Phys. Chem*. **1991**, *95*, 3480.
(30) El-ghayoury, A.; Harriman, A.; Ziessel, R. *Chem. Commun*. **1999**, 2027.
(31) Decurtins, S.; Felix, F.; Ferguson, J.; Güdel, H. U.; Ludi, A. *J. Am. Chem. Soc*. **1980**, *102*, 4102.
(32) Marcus, R. A.; Sutin, N. *Biochim. Biophys. Acta* **1985**, *811*, 265.
(33) Schlicke, B.; Belser, P.; De Cola, L.; Sabbioni, E.; Balzani, V. *J. Am. Chem. Soc*. **1999**, *121*, 4207.
(34) Förster, T. *Discuss. Faraday Soc*. **1959**, *27*, 7.
(35) (a) Oevering, H.; Verhoeven, J.; Paddon-Row, M. N.; Cotsaris, E. *Chem. Phys. Lett*. **1988**, *143*, 488. (b) Oliver, A. M.; Craig, D. C.; Paddon-Row, M. N.; Kroon, J.; Verhoeven, J. *Chem. Phys. Lett*. **1988**, *150*, 366.
(36) Razi Naqvi, K.; Steel, C. *Spectrosc. Lett*. **1993**, *26*, 1761.
(37) Grosshenny, V.; Harriman, A.; Hissler, M.; Ziessel, R. *J. Chem. Soc., Faraday Trans*. **1996**, *92*, 2223.
(38) Juris, A.; Prodi, L.; Harriman, A.; Ziessel, R.; Hissler, M.; El-ghayoury, A.; Wu, F.; Riesgo, E. C.; Thummel, R. P. *Inorg. Chem*., in press.
(39) Heitele, H.; Finckh, P.; Weeren, S.; Pöllinger, F.; Michel-Beyerle, M. E. *J. Phys. Chem*. **1989**, *93*, 5173.
(40) Osuka, A.; Marumo, S.; Mataga, N.; Taniguchi, S.; Okada, T.; Yamazaki, I.; Nishimura, Y.; Ohno, T.; Nozaki, K. *J. Am. Chem. Soc*. **1996**, *118*, 155.
(41) McConnell, H. H. *J. Chem. Phys*. **1961**, *35*, 508.